

BRIEF REPORTS AND COMMENTS

This section is intended for the publication of (1) brief reports which do not require the formal structure of regular journal articles, and (2) comments on items previously published in the journal.

Fabrication of nickel oxide nanostructures by atomic force microscope nano-oxidation and wet etching

Ju-Hung Hsu, Hsin-Wen Lai, Heh-Nan Lin,^{a)} Chia-Chih Chuang, and Jin-Hua Huang
Department of Materials Science and Engineering, National Tsing Hua University, Hsinchu 300, Taiwan

(Received 20 June 2003; accepted 2 September 2003; published 26 November 2003)

We report the fabrication of nickel oxide nanostructures by atomic force microscope nano-oxidation and subsequent wet etching. By applying a negative bias to a conductive tip, nickel oxide patterns are first created by the process of nano-oxidation. The unoxidized nickel film is then etched away in a diluted nitric acid solution. Auger electron spectroscopy measurements confirm the complete removal of the nickel film and the preservation of the oxide patterns. Nickel oxide nanodots with diameters as small as 100 nm are reliably produced by the present method. © 2003 American Vacuum Society. [DOI: 10.1116/1.1621655]

Scanning probe lithography (SPL) has been used extensively in recent years to create nanostructures or nanodevices below the 100 nm scale.¹ Among the various SPL techniques, one of the most adopted methods is the anodic nano-oxidation. The process is usually realized by applying a negative bias to the tip in an atomic force microscope (AFM) under ambient conditions. The high field between the tip and the sample leads to the decomposition of the water layer and the oxidation of the sample underneath the tip. The nano-oxidation of silicon has so far been the most studied.²⁻⁵ The nano-oxidation of metals such as chromium,⁶ titanium,^{7,8} aluminum,⁹ and molybdenum¹⁰ have also been demonstrated. One of the applications of metal oxide nanostructures is used as masks in lithographic procedures.

The nano-oxidation of nickel has not been reported and nickel oxide nanostructures are valuable for the following reasons. In addition to being used as a mask material, the created nanostructures can be potentially used for nano-optoelectronic devices since nickel oxide is a well-known electrochromic material.^{11,12} Besides, the oxide may be reduced to nickel in a reactive gas environment. The resultant nickel nanopatterns can be used for nanomagnetic studies or catalytic growth of nanomaterials. In this Brief Report, nickel oxide nanostructures are created by AFM nano-oxidation and subsequent wet etching. Nanodots with diameters as small as 100 nm were successfully produced.

The nickel film was prepared by electron beam evaporation onto silicon substrates with a thick thermal oxide. The film thickness and root-mean-square roughness were around 15 and 0.13 nm, respectively. The experiment was performed in a commercial atomic force microscope (Smena-A, NT-MDT, Russia) under ambient conditions with humidity of

around 50%. The nano-oxidation was realized by applying a negative bias to the tip with the sample grounded. Two types of cantilevers were used in the experiment. One is a rectangular silicon cantilever (CSC12, Micro Masch, Russia) and the other is a triangular silicon cantilever coated with tungsten carbide (NSC11, Micro Masch, Russia). Contact and intermittent contact AFM operation modes were both employed.

By varying the voltage (negative) applied to the tip, it was found that nickel oxide was not produced when the magnitude was below 5 V but consistently generated when above that value. On the other hand, uncontrollable large features were produced when the magnitude was above 10 V. By scanning a silicon tip in the contact mode operation with a bias of -8 V, a $3 \times 3 \mu\text{m}^2$ nickel oxide square was created and the image is shown in Fig. 1(a). The oxide height is 60 nm, or four times more than the original film thickness. In addition, the oxidized surface becomes much rougher with large grains as is clear in the figure. The sample was then dipped into a solution of 14% nitric acid to remove the nickel. For a time of more than 70 s, a visible change of sample color was observed and indicated the removal of nickel. After being rinsed with de-ionized water, the sample was imaged again and the same oxide square is shown in Fig. 1(b). Evidently, the oxide pattern was not affected by the wet etching.

To verify if the nickel was completely etched, the sample was analyzed by Auger electron spectroscopy (AES) (Auger 670 PHI Xi, Physical Electronics, U.S.A.). The AES spectra shown in Figs. 2(a) and 2(b) were taken on the unoxidized nickel surface before and after etching, respectively. In Fig. 2(a), the nickel peaks at around 800 eV and the oxygen peak at 500 eV indicate that the original nickel surface composition was native nickel oxide. In Fig. 2(b), the disappearance of the nickel signals and the occurrence of silicon peak at

^{a)}Author to whom correspondence should be addressed; electronic mail: hnlin@mse.nthu.edu.tw

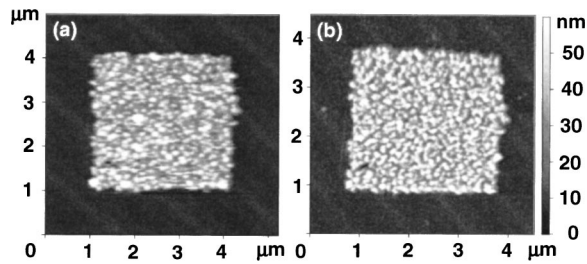


FIG. 1. AFM images of a $3 \times 3 \mu\text{m}^2$ nickel oxide square (a) before and (b) after wet etching. The pattern was created with a tip bias of -8 V in contact mode operation.

1600 eV confirm that the original nickel was completely removed after wet etching. On the other hand, the spectra taken on the oxide pattern before and after the wet etching as shown in Figs. 2(c) and 2(d), respectively, are almost unchanged. The results indicate the wet etching had little effect on the oxide. In addition, a comparison between the oxygen peaks in Figs. 2(a) and 2(c) also reveals the effectiveness of the AFM nano-oxidation since the oxygen signal is stronger in the latter figure.

By locating the tip at desired locations without scanning and using single voltage pulses, single nickel oxide nanodots were successfully created. Better reproducibility, however, was achieved by the intermittent contact mode. The advantages of this operation mode have been discussed in the literature.^{3,8} By using a tungsten carbide coated silicon tip, a 3×3 nickel oxide nanodot array was created with the application of -8 V , 500 ms pulses. The scanning electron microscope (SEM) (JSM-6500F, JEOL, Japan) image is shown in Fig. 3(a), and the average dot diameter is around 100 nm.¹³

The nanodot array also survived the same etching process as mentioned previously and the resulting SEM image is shown in Fig. 3(b). Therefore, the present method can at least produce nickel oxide nanostructures of sizes around 100 nm. Smaller nanodots were also created with pulses of shorter durations, but they were not preserved after the etch-

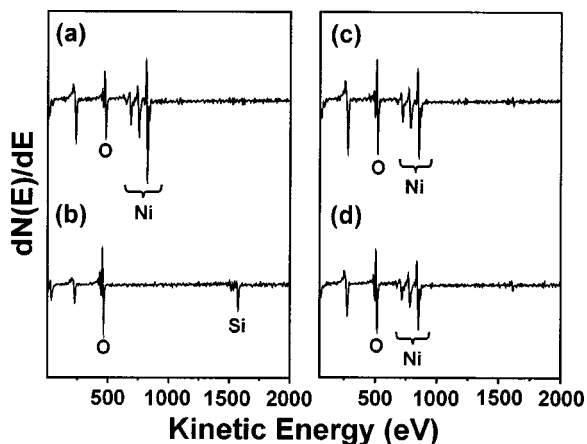


FIG. 2. AES spectra on the same sample as in Fig. 1. (a) and (b) were obtained on nickel before and after etching, respectively. (c) and (d) were obtained on the oxide pattern before and after etching, respectively.

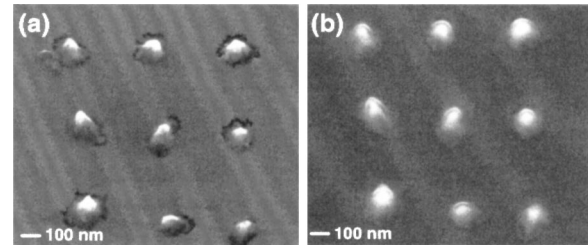


FIG. 3. SEM images of nickel oxide nanodots (a) before and (b) after wet etching. The nanodots were created with the application of -8 V , 500 ms pulses in intermittent contact mode operation.

ing process. The origin was probably due to incomplete oxidation of nickel. With the use of thinner films, it is expected that nanodots of sizes less than 100 nm will survive the wet etching. In addition, the tungsten carbide tips have large diameters and smaller features are therefore possible with sharper tips. Furthermore, if the oxide nanostructures undergo a chemical reduction, the created nickel structures are guaranteed to have finer sizes.

The mechanism of AFM nano-oxidation has not been completely understood at present time. Nevertheless, the following equations are found to describe the growth kinetics well:^{2,4,5}

$$\frac{dh}{dt} = R \exp\left(\frac{-h}{h_0}\right), \quad (1)$$

$$h = h_0 \ln\left(\frac{R}{h_0}t + 1\right), \quad (2)$$

where h is the oxide height, t the pulse duration, h_0 the characteristic height, and R the maximum rate. The growth rate dh/dt is equal to the oxide height divided by the pulse duration, and Eq. (2) is a direct integration of Eq. (1). Four

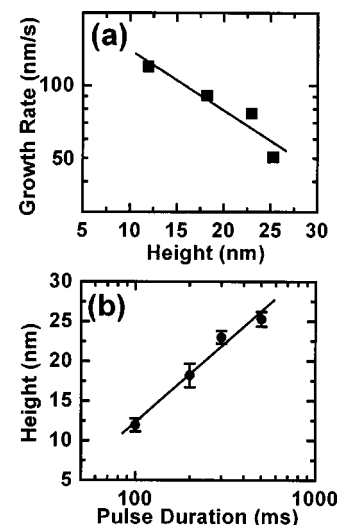


FIG. 4. (a) Growth rate vs oxide height and (b) oxide height vs pulse duration relationships obtained with -8 V pulse of durations 100, 200, 300, and 500 ms.

different pulse durations were tested with the voltage maintained at -8 V, and the relationship between the growth rate and the oxide height is plotted in Fig. 4(a). From the linear fit, R and h_0 are equal to 250 nm/s and 17.4 nm, respectively. The relationship between the oxide height and the pulse duration is also shown in Fig. 4(b). By ignoring the additive term in Eq. (2), a linear fit gives 360 nm/s and 8.7 nm for R and h_0 , respectively. Since the present oxide heights are larger than 10 nm, the later results are probably more reliable. The detail, however, would need further investigation.

To summarize, nickel oxide nanostructures with sizes down to 100 nm were successfully fabricated by AFM nano-oxidation and subsequent wet etching in a nitric acid solution. The AES spectra on the samples before and after the etching ascertain the removal of original nickel and the survival of nickel oxide. Potential applications of the created nanostructures include lithographic masks, nanomagnetic studies, and patterned growth of nanomaterials.

The authors acknowledge the AES measurements at the NTHU Instrument Center. This work was supported by the National Science Council under Grant No. 91-2120-E-007-

001 and the Ministry of Education, Program of Academic Excellence under Grant No. A-91-E-FA04-1-4.

¹H. T. Soh, K. W. Guarini, and C. F. Quate, *Scanning Probe Lithography* (Kluwer, Boston, 2001).

²Ph. Avouris, T. Hertel, and R. Martel, *Appl. Phys. Lett.* **71**, 285 (1997).

³R. Garcia, M. Calleja, and H. Rohrer, *J. Appl. Phys.* **86**, 1898 (1999).

⁴E. S. Snow, G. G. Jernigan, and P. M. Campbell, *Appl. Phys. Lett.* **76**, 1782 (2000).

⁵J. A. Dagata, F. Perez-Murano, G. Abadal, K. Morimoto, T. Inoue, J. Itoh, and H. Yokoyama, *Appl. Phys. Lett.* **76**, 2710 (2000).

⁶D. Wang, L. Tsau, K. L. Wang, and P. Chow, *Appl. Phys. Lett.* **67**, 1295 (1995).

⁷E. S. Snow and P. M. Campbell, *Science* **270**, 1639 (1995).

⁸B. Irmer, M. Kehrle, and J. P. Kotthaus, *Appl. Phys. Lett.* **71**, 1733 (1997).

⁹E. S. Snow, D. Park, and P. M. Campbell, *Appl. Phys. Lett.* **69**, 269 (1996).

¹⁰M. Rolandi, C. F. Quate, and H. Dai, *Adv. Mater. (Weinheim, Ger.)* **14**, 191 (2002).

¹¹A. Azens and C. G. Granqvist, *J. Solid State Electrochem.* **7**, 64 (2003).

¹²K.-S. Ahn, Y.-C. Nah, and Y.-E. Sung, *J. Vac. Sci. Technol. A* **20**, 1468 (2002).

¹³Because the tungsten carbide tip had a large diameter of around 100 nm, the obtained AFM image could not be used for a good determination of the dot size.